INNO-U-01

Validation of a groundwater flow and transport modeling tool for borehole thermal energy stores based on FEFLOW

Dan Bauer[1,2], Wolfgang Heidemann[1], Harald Drück[1,2]

[1]University of Stuttgart, Institute of Thermodynamics and Thermal Engineering (ITW), [2]Research and Testing Centre for Thermal Solar Systems (TZS), Pfaffenwaldring 6, 70550 Stuttgart, Germany,
Phone: +49-711-68569445,Fax: +49-711-68563503, e-mail: bauer@itw.uni-stuttgart.de

1. Introduction

The thermal performance of borehole thermal energy stores (BTES) used for seasonal balancing of heat gained by large solar thermal systems or by combined heat and power generation (CHP) systems is sensitive to groundwater flow. Hence, the storage utilization ratio and the required size of the store and so the number and length of the borehole heat exchangers (BHE) that mainly govern the installation costs depend on the undergrounds hydrogeological condition. In recent years, a numerical mass and heat transport model has been developed at the Institute of Thermodynamics and Thermal Engineering (ITW), University of Stuttgart, together with the German company DHI-WASY GmbH (the software developer of FEFLOW [1]). The model has been developed in order to simulate the thermal behavior of complete large scale solar thermal or CHP systems combined with BTES as one key element to contribute to an increase of the number of potential sites through increased planning reliability [2], [3], [4]. This paper presents the validation of the developed model against an analytical solution and measured data of two BTES with and without groundwater flow.

2. Materials and method

Model description: The developed numerical simulation model is an add-on to the finite-element ground water flow and transport modeling tool FEFLOW. Several two-dimensional thermal resistance and capacity models (TRCM) [5] were connected to a three-dimensional BHE model capable of describing all relevant transient heat and mass transport processes inside the borehole. This BHE model then was coupled as a one-dimensional line element to the three-dimensional finite element mesh representing the underground [2], [3], [4], see Figure 1. Multiple BHE can be set. The underground elements next to the BHE line element must have a particular size. An iterative method based on Lord Kelvin's line source theory has been developed to size them [4]. A detailed and comprehensive description of the FEFLOW model can be found in [2].

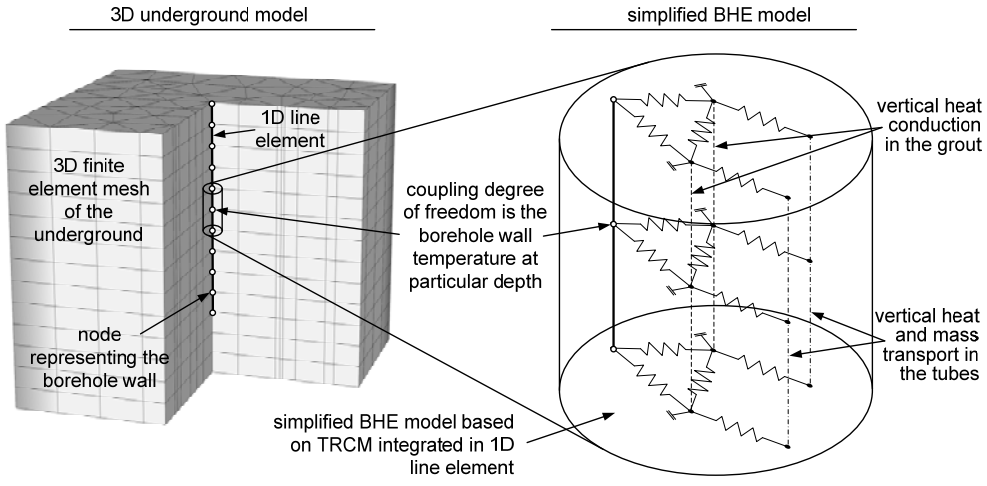

Figure 1: Numerical BHE simulation model based on TRCM integrated in one-dimensional line element which itself is coupled to a three-dimensional finite element mesh representing the underground

Model validation 1: The FEFLOW model is compared to an analytical solution which is an extension of Lord Kelvin's line source theory by a constant movement of the line source. It is known in literature as "moving line source theory". It can also be applied to a BHE that is influenced by moving groundwater where the heat source BHE is locally fixed and the liquid part of the underground moves instead [6], [7], [8]. This analytical solution offers short computation times but it is limited to a two-dimensional horizontal description of the combined heat and mass transport process in the underground surrounding a BHE. Vertical heat conduction in the underground cannot be considered. Hence, computation results should be regarded by keeping these assumptions in mind.

To ensure accurate computation results of the FEFLOW model, the following criteria must be verified:

- the time-dependent fluid temperature in the tubes and the borehole wall temperature for different groundwater velocities
- the time-dependent underground temperature around a BHE with groundwater flow
- the time-dependent underground temperature around several BHE in thermal interaction.

Sutton et al. [6] gives an explicit solution for the horizontal underground temperature around a BHE:

$$\vartheta_s(Fo,x,y)=\frac{\dot{q}}{4\pi\cdot k_{eff}}\cdot e^{\frac{Pe\cdot x}{d_b}}\cdot\int_{\frac{x^2+y^2}{Fo\cdot {d_b}^2}}^{\infty}\xi^{-1}e^{-\xi-\frac{Pe^2(x^2+y^2)}{4{d_b}^2\xi}}d\xi+\vartheta_{s,0} \quad (1)$$

where

$$Fo=\frac{4a_{eff}\cdot t}{{d_b}^2} \quad (2) \qquad Pe=\frac{w_{eff}\cdot d_b}{2a_{eff}} \quad (3)$$

$$a_{eff}=\frac{k_{eff}}{[\Omega\cdot\rho_f c_{p,f}+(1-\Omega)\rho_s c_{p,s}]} \quad (4) \qquad k_{eff}=\Omega\cdot k_f+(1-\Omega)k_s \quad (5)$$

$$w_{eff}=\frac{\Omega\cdot\rho_f c_{p,f}}{[\Omega\cdot\rho_f c_{p,f}+(1-\Omega)\rho_s c_{p,s}]}\cdot w_a \quad (6) \qquad w_a=\frac{w_{DA}}{\Omega} \quad (7)$$

x is the distance from the BHE in downstream direction, y is the distance at right angles to the flow direction. Chaudhry and Zubair [11] define a function named "generalized incomplete gamma function" to characterize the semi-infinite integral in (1) for what no closed-form solution exists:

$$\Gamma(a,x_\Gamma;b)=\int_{x_\Gamma}^{\infty}\xi^{a-1}e^{-\xi-\frac{b}{\xi}}d\xi \quad (8)$$

Equation (1) can now be expressed as follows:

$$\vartheta_s=\frac{\dot{q}}{4\pi k_{eff}}\cdot e^{\frac{Pe\cdot x}{d_b}}\cdot\Gamma\left(0,\frac{x^2+y^2}{{d_b}^2 Fo};\frac{Pe^2(x^2+y^2)}{4{d_b}^2}\right)+\vartheta_{s,0} \quad (9)$$

The "generalized incomplete gamma function" can be numerically evaluated by using the following series expansion which only converges for small values of b (viz. near the BHE) and for small Péclet-Numbers [11]:

$$\Gamma(0,x_\Gamma;b)={}_0F_1(-,1;b)\cdot E_i(x_\Gamma)+\sum_{n=1}^{\infty}\left[\frac{b_n}{(n!)^2}\sum_{m=0}^{n-1}m!\left(\frac{-1}{x_\Gamma}\right)^{m+1}\right] \quad (10)$$

Chaudhry et al. [12] give more asymptotic expansions for different ranges of the parameters.

There is a special interest in evaluating the temperature at the borehole wall ($x^2+y^2=0.25{d_b}^2$). It can be obtained through averaging by integrating in circumferential direction [6]:

$$\vartheta_b(Fo)=\frac{\dot{q}}{4\pi k_{eff}}\cdot I_0\left(\frac{Pe}{2}\right)\cdot\Gamma\left(0,\frac{1}{4Fo};\frac{Pe^2}{16}\right)+\vartheta_{s,0} \quad (11)$$

Based on the borehole wall temperature, the average temperature of the fluid can be obtained by adding the steady state temperature difference between fluid and borehole wall:

$$\vartheta_f(Fo) = \frac{\dot{q}}{4\pi k_{eff}} \cdot I_0\left(\frac{Pe}{2}\right) \cdot \Gamma\left(0, \frac{1}{4Fo}; \frac{Pe^2}{16}\right) + \vartheta_{s,0} + \frac{\dot{q}}{R_b} \qquad (12)$$

The validation was carried out with a 40 m long single U-tube BHE. Table 1 lists geometrical data, operating conditions, physical property and the BHE thermal resistance of the calculations.

Table 1: Data of the comparative calculations

geometrical data			operating conditions			thermal resistance physical property		
d_i	(mm)	26.2	$\dot{m}$	(kg s^{-1})	0.25	R_b	(K m W^{-1})	0.096
d_o	(mm)	32	$\dot{q}$	(W m^{-1})	50	k_{eff}	(W K^{-1} m^{-1})	2.184
d_b	(mm)	130	$\vartheta_{s,0}$	(°C)	10			

Model validation 2: The numerical model is validated against underground temperatures and the fluid outlet temperature of the Neckarsulm experimental BTES [9] measured during a three month test run. The underground at this site consists of layers of different claystones above limestone. The layers between the ground surface and some meters below the lower end of the BHE have a very low hydraulic conductivity, so there is no groundwater flow at this site. More information on the local geology and hydrogeology can be found in [9].

The first section of the Neckarsulm BTES was built in 1997 as an experimental BTES. Several simulation models have already been validated against this BTES [9], [13]. The BTES consists of 36 double-U-tube BHE installed at two-meter intervals. Six BHE each are hydraulically connected in series. The BHE were installed in boreholes with a diameter of 115 mm and a depth of 30 m resulting in a store volume of some 4 300 m^3. The underground temperature can be measured in three additional boreholes inside and outside the borefield at different depths. Figure 2 depicts the BTES configuration.

A three-dimensional FEFLOW model of the Neckarsulm BTES was set up. The extension of the finite element model in horizontal and vertical direction was chosen sufficiently large to avoid boundary influences during computation. Finite elements near the boreholes are small while the element size increases outside the BTES. The FEFLOW model consists of 205 728 elements in total. Figure 3 depicts the finite element mesh.

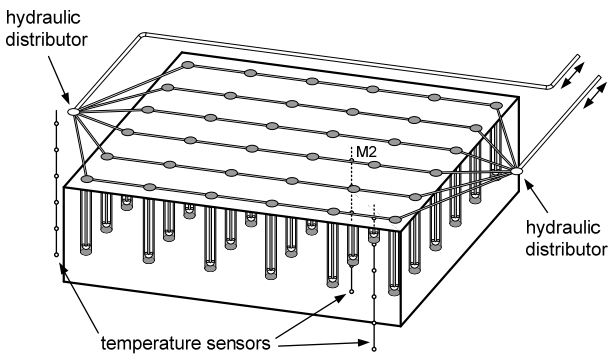

Figure 2: Configuration of the Neckarsulm experimental BTES [14]

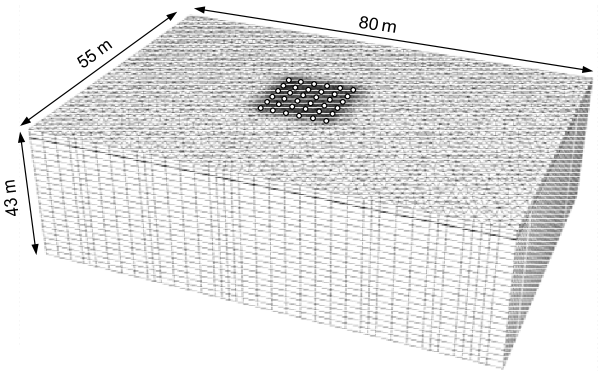

Figure 3: Finite element mesh of the Neckarsulm BTES model

Like the other BTES model validations described in [9] and [13], the thermophysical properties of the underground ($\rho_s \cdot c_{p,s}$ = 3 000 kJ m^{-3} K^{-1}, k_s = 2 W m^{-1} K^{-1}) were taken from [15]. They have been determined by numerical parameter identification based on measured data and suppose a homogenous underground. Table 2 lists geometrical data and physical properties of one BHE being representative for all 36 BHE [13], [16].

Table 2: Geometrical data and physical properties of the BHE [13], [16].

geometrical data			physical properties		
d_i	(mm)	20,4	$\rho_p \cdot c_{p,p}$	(J m^{-3} K^{-1})	1,82·10^6
d_o	(mm)	25,0	k_p	(W m^{-1} K^{-1})	0,22
d_b	(mm)	115	$\rho_g \cdot c_{p,g}$	(J m^{-3} K^{-1})	3,587·10^6
s	(mm)	65,0	k_g	(W m^{-1} K^{-1})	0,65
L	(m)	30,0	heat transfer fluid is pure water		

The BHE are covered with a 200 mm thick thermal insulation layer made of extruded polystyrene ($\rho \cdot c_p$ = 35 kJ m^{-3} K^{-1}, k = 0,04 W m^{-1} K^{-1}) which extends two meters beyond the outermost BHE. This thermal insulation as well as a 2,5 m thick soil cover layer on top of the insulation were thoroughly modeled.

Model validation 3: The numerical model is validated against measured data of a two years period of operation of the BTES in Crailsheim. This BTES [10] is influenced by moving groundwater in one aquifer and several aquitards. The BTES was constructed in 2008. It was built as major part of a solar district heating system [19]. The BTES consists of 80 double U-tube BHE, which were drilled to 55 m depth in a distance of 3 m to each other within a circular area of 30 m diameter. Each BHE is installed in a 0.13 m borehole and is cemented with grout of Stüwatherm. The BTES is covered with a 0.4 m thick thermal insulation material and 1.6 m soil from nearby earthworks. The BTES in Crailsheim operates with pure water as heat transfer fluid. BHEs are interconnected by pairs, with one BHE being situated rather inside of the BHE grid and one more outside, see Figure 4. The flow direction of the heat transfer fluid is from the inner BHE to the outer during charging and the other way round during discharging of the BTES.

The BTES is monitored in detail: The flow rate within the pipes from and to the heat store as well as the in- and outlet temperatures are logged permanently during the operation of the system. Based on this data the heat amount transferred to the store during charging and removed from the store during discharging can be calculated. Furthermore, 24 temperature sensors have been installed at 12 different depths on the measuring lances M1 and M31, see Figure 4. Both measuring lances record temperatures of the solid underground up to a depth of 80 m. In addition, groundwater temperatures and levels are measured in the wells GWM2, GWM3 and GWM4 80 m below ground surface (aquifer in the Upper Muschelkalk) and in the wells GWM2a, GWM3a and GWM4a 20 m below ground surface (aquitards in the Lower Keuper), see Figure 4.

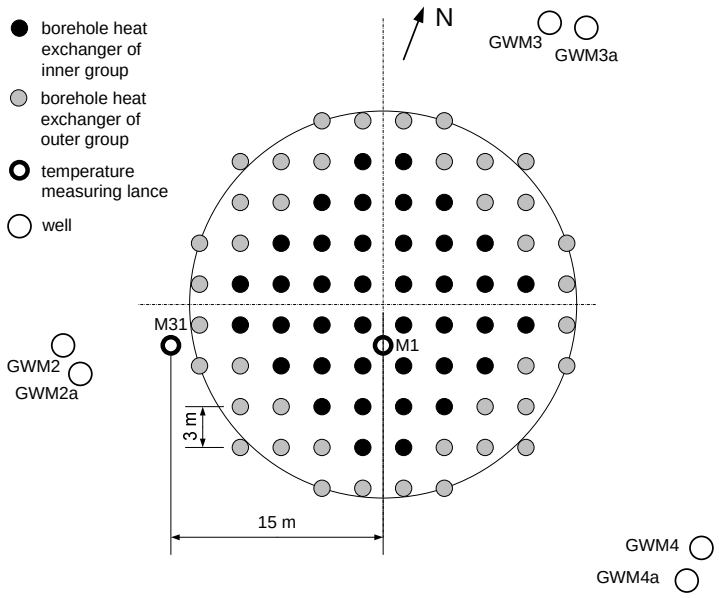

Figure 4: Layout of the Crailsheim BTES with position of BHE, wells and temperature measuring lances

Pumping and recharge tests conducted at the six wells returned transmissivities between 5.1·10^{-5} m^2 s^{-1} and 1.9·10^{-7} m^2 s^{-1}. The determined storage coefficients imply unconfined groundwater conditions for the aquifer in the Upper Muschelkalk and confined conditions for the aquitards in the Lower Keuper [20].

The simulation model is based on three 80 m core sections drilled at the project site. The cores have been analysed in detail with respect to lithology, facies and thermal and hydraulic parameters [20]. The thermal conductivity, specific heat capacity and permeability have been measured on 76 representative samples using pointwise measurement techniques. Additionally, the main joint directions have been recorded in two reference outcrop sections and have been incorporated into the model [20]. In general, the geological and hydrogeological settings at the site are very suitable for validating the FEFLOW BTES model. Especially the low, but still measurable groundwater flow through the BTES and the aquifer below the BTES with its higher flow rate enable the investigation of the thermal effect of a BTES on the subsurface.

The model dimension extends over 1.5 km in downstream direction and 500 m in upstream direction of the aquifer [20]. The width was set to 1 km, with the BTES being placed in the middle. The depth of the model was set to -150 m with the BTES ranging from 0 to -55 m. Model layers and their thickness have been chosen individually to fit the geological realities. However, the intensely interbedded structure with layers often changing every few centimeters could not be modeled in detail. Consequently, multiple single geological layers had to be merged to reasonable model layers [20]. The maximum discretization level for the vertical element heights was set to 1 m, the minimum to 10 m. Generally, layers in the vicinity of the BTES (i.e. the topmost 75 m) have a thickness of 1 to 4 m, while layers far below the BTES have 5 to 10 m thickness. The covering of the BTES, consisting of thermal insulating material (0.4 m) and soil from nearby earthworks (1.6 m) was modeled by two additional continuous layers that taper off to 0.01 m each outside the BTES. The predefined mesh sizes changes with distance to the BTES. Element sizes around each individual BHE are finest with horizontal triangle areas of 0.02 to 0.08 m², increases to 0.1 to 0.4 m² in the space between the BHE, increases further to 0.5 to 2 m² in an oval shaped area that encloses the BTES and points in down-stream direction, and has its coarsest elements (200 to 500 m²) in the remaining area. The total model consists of 58 layers and about 1 445 000 finite elements. The dimensions are shown in Figure 5.

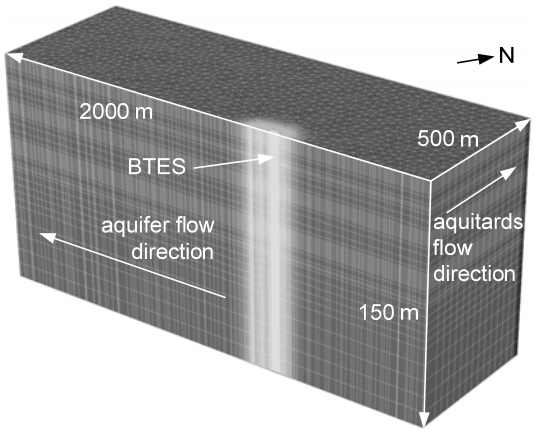

Figure 5: Model and layer dimensions of the 3D-finite element mesh (vertical cut through the middle of the BTES along the aquifer flow direction); vertical exaggeration: 5x

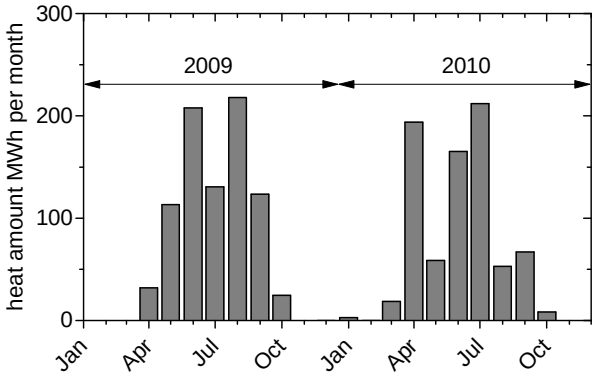

Figure 6: Measured amount of heat transferred to the BTES

Groundwater flow directions were defined by setting suitable hydraulic heads as 1st kind boundary condition at the model borders [20]. The hydraulic gradient of the aquitards was set to 0.01, while the aquifer has 0.0045. Basing on the prior merged geological layers averaged hydraulic conductivities have been assigned to the individual model layers. Flow rates within the aquifer and aquitards are primary controlled by fractures, thus known literature values from the Bavarian Environment Agency have been used here. Subsequently, the simulation was run in steady mode with flow calculation only to obtain suitable initial hydraulic conditions for the following unsteady heat transport simulation. For the heat transport simulation the necessary parameters such as porosity, thermal conductivity and heat capacity have been assigned to the individual layers. While the thermal conductivity and heat capacity values could be taken directly from the measurement results, the porosity had to be converted first. The measured values are the gas-effective porosity, while FEFLOW needs the water-effective

porosity. Thus, porosities had to be significantly reduced. To retain the relative porosities differences of the different measured rocks all porosities have been decreased based on experience by factor five. So, the resulting porosities fit quite well to known values from literature. The initial temperature distribution of the model has been calculated by using a fixed surface temperature of 10.5 °C and a heat inflow of 0.065 W m^{-2} at the base of the model. The resulting temperature gradient is about 3.5 K per 100 m depth. The 80 BHE have been integrated as 4^{th} kind boundary condition with data for the grout and the pipes according to the manufacturers. After setting up all required BHE parameters all BHE were interconnected pairwise using FEFLOW's internal BHE Integrator.

The transient simulation was conducted over two years in order to validate FEFLOW against measured data of a two years period of operation. During this two year period the BTES was only charged and no active discharging was performed. Heat removal from the BTES only took place due to heat losses and ground water flow. The measured amount of heat transferred to the BHE was set as boundary condition to the model, see Figure 6. For the validation the computed and measured temperatures at measuring lances M1 and M31 as well as groundwater temperatures at GWM2a–4a and GWM2–4 were compared.

3. Results and discussion

Model validation 1: Figure 7 depicts the average fluid temperature and borehole wall temperature against Fourier number for different Péclet numbers calculated with the analytical and the FEFLOW model. Here, $Fo = 10^6$ corresponds to 136.7 years. $Pe = 0$ means resting groundwater, Pe = 1 corresponds to a Darcy velocity of $w_{DA} = 0.703$ m/d.

As can be seen, the calculation results of the different models match very well. The steady state conditions are reached after the same amount of time and converge towards the same value. A steady state condition can only be reached for $Pe > 0$.

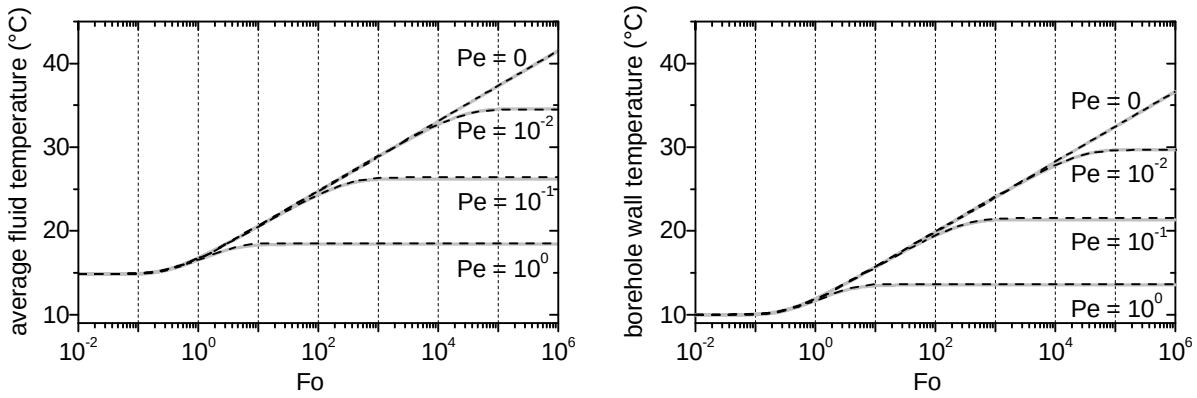

Figure 7: Comparison of the average fluid temperature (left) and borehole wall temperature (right) calculated with the FEFLOW model (dashed black lines) and the analytical model (solid gray lines)

Figure 8 shows the calculated horizontal temperature of the underground around a BHE for $Pe = 0.05$. Again, a very good match between the FEFLOW model and the analytical model can be stated. The differences at $Fo = \infty$ might result from the different model dimensions. While the analytical model is two-dimensional horizontal, the FEFLOW model is three-dimensional and includes vertical heat conduction. The shown temperatures calculated with the FEFLOW model are averaged over depth. While the temperature profile extends in horizontal direction, it changes shape from a cylinder towards a sphere. Hence, vertical heat conduction influences the isotherms. This effect can't be considered by the analytical model.

Figure 9 shows the calculated horizontal temperature of the underground around a field of six BHE for $Pe = 0.05$ and $Pe = 0$ at $Fo = 1000$. Six BHE line elements were integrated in FEFLOW's three-dimensional finite element mesh which automatically accounts for the thermal interaction. The solution of the analytical model can be obtained by local superposition of the temperature fields of all six BHE. Both methods lead to very similar results.

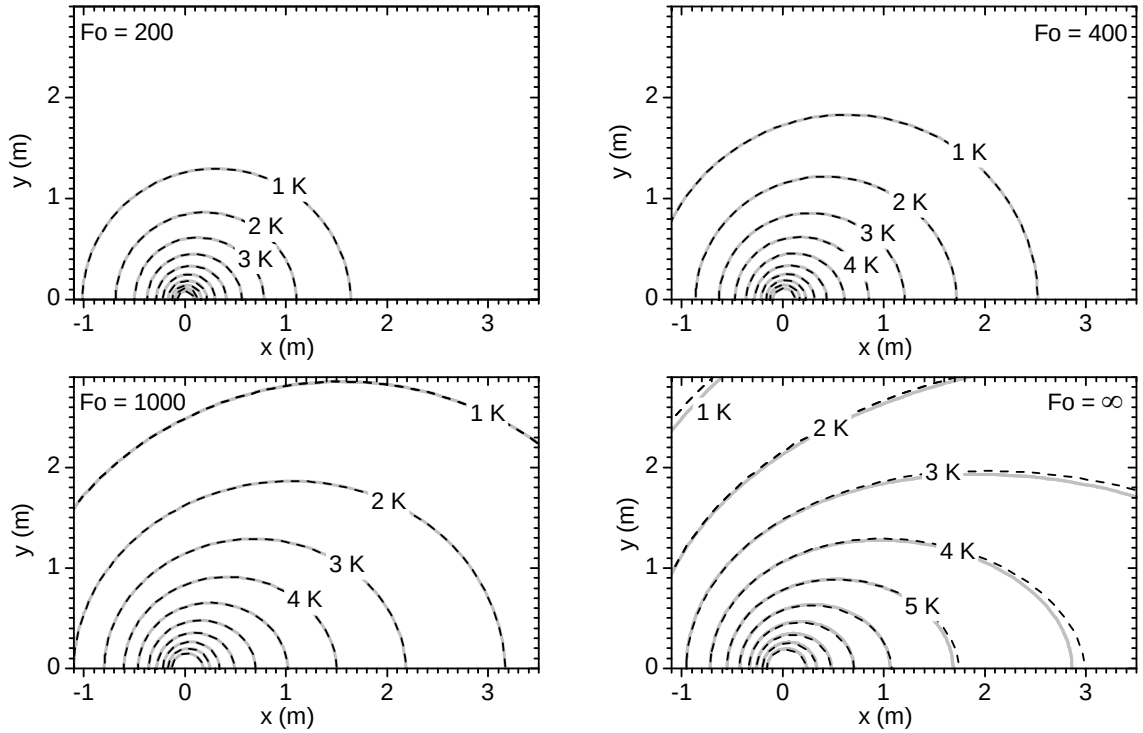

Figure 8: Horizontal temperatures of the underground around a BHE for Pe = 0.05 at different Fourier numbers; FEFLOW model: dashed black lines; analytical model: solid gray lines; isotherms with 1 K up to 10 K above initial underground temperature are depicted

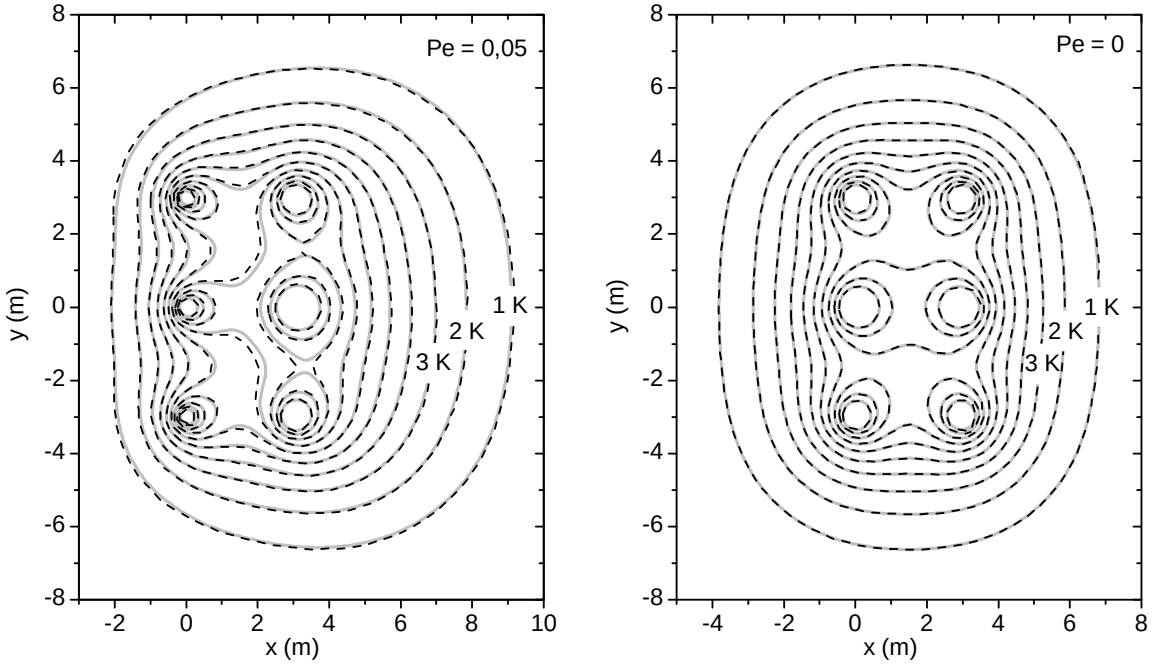

Figure 9: Horizontal temperature of the underground around a field of six BHE for Pe = 0.05 and Pe = 0 at Fo = 1000; FEFLOW model: dashed black lines; analytical model: solid gray lines; isotherms with 1 K up to 10 K above initial underground temperature are depicted

Model validation 2: The BTES was charged from December 17th 1997 till March 4th 1998 with an inlet temperature between 65 °C and 80 °C and a flow rate of about 12 m^3 h^{-1}. Underground temperatures up to 53 °C were reached in the middle of the BTES at the end of the charging period [14]. Afterwards a discharging period of three weeks followed with a flow rate of about 3 m^3 h^{-1} and an inlet temperature between 40 °C and 50 °C.

The measured flow rate and inlet temperature were set as time-varying boundary conditions to the FEFLOW model. Then, the computed BTES outlet temperature and the computed underground temperature at a depth of 20 m at position M2 (see Figure 2) were compared to the measured values. Figure 10 shows the comparison of computed and measured temperatures.

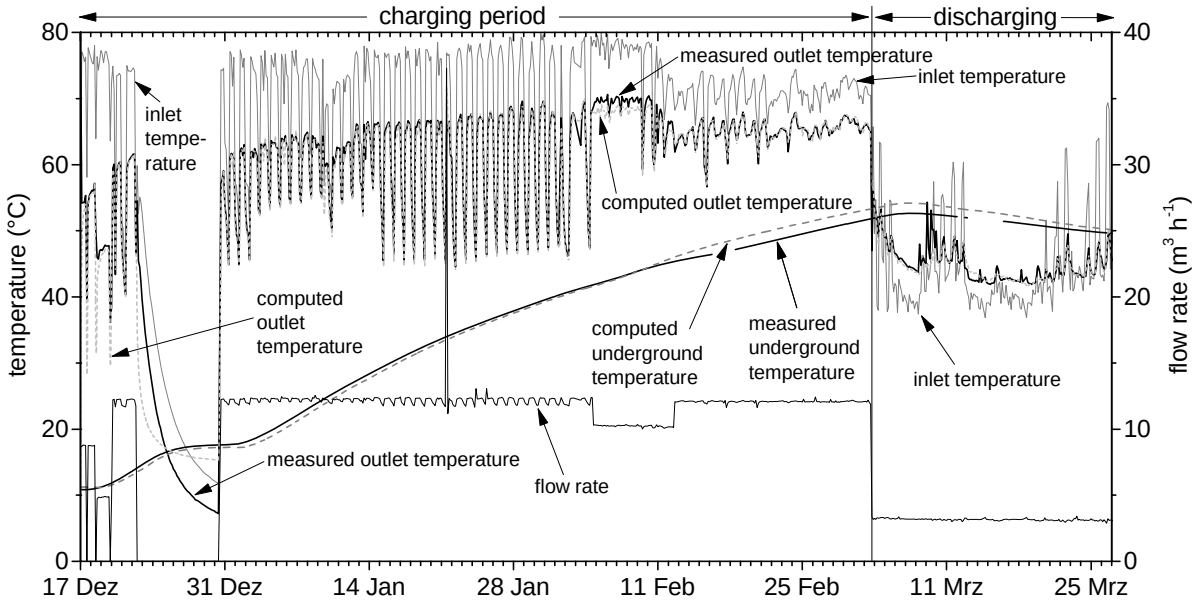

Figure 10: Comparison of computed and measured temperatures of the Neckarsulm experimental BTES

During the first week of the charging period small differences between measured and computed values occur. This might be explained by small deviations between the real initial temperature distribution of the underground and the one set to the model. From 31st of December until the end of the charging period measured and computed values match very well with some exceptions. On February 4th the flow rate was reduced to about 10 $m^3 h^{-1}$. It was raised back to about 12 $m^3 h^{-1}$ on February 12th. A difference of 1–2 K between measured and computed BTES outlet temperature can be noticed. However, this difference disappears after the increase of the flow rate. During the discharging period computed and measured values match very well. Only on March 9th and 10th small differences occur. The computed underground temperature at a depth of 20 m fits very well to the measured one until February 11th. Afterwards the computed temperature exceeds the measured temperature by about 1 K. During the following discharging period computed and measured underground temperatures converge.

The computation results of the FEFLOW model can be considered as very good, except for the few differences described. In addition, the computation results match very well the computations made by other scientists [9], [13] with the simulation model TRNSBM [17] and a fully discretized numerical ANSYS model [18]. One reason for the described differences in the BTES outlet temperatures is the deviation between the real initial temperature distribution of the underground and the one set to the FEFLOW model. One more reason is the quality of the measured data: Some data points were missing and had to be interpolated. The strong increase of the flow rate to 37 $m^3 h^{-1}$ on January 21st is attributed to a malfunction of the data acquisition system. The decrease of the flow rate during February 4th and 12th and the simultaneous difference between measured and computed outlet temperatures is attributed to a blockage of a row of six BHE. The mismatch of measured and computed underground temperature after February 11th is considered as a consequence of this blockage.

Model validation 3: Figures 11 and 12 depict the comparison between measured and computed underground temperatures at measuring lances M1 (middle of the BTES) and M31 (margin of the BTES), see Figure 4. Figures 13 and 14 depict the comparison between measured and computed groundwater temperatures at wells GWM2a–4a (20 m depth) and GWM2–4 (80 m depth). The gaps in the curves representing the measured data in Figures 13 and 14 are due to failures of the data acquisition system. The bulky appearance of these curves is caused by measurement noise.

Both, the temperatures of the solid ground and the groundwater can be properly computed with the FEFLOW model. Minor differences have to be accepted because of the following reasons: The measured amount of heat transferred to the BTES and set as boundary condition to the model is slightly too high because it includes the unknown thermal losses of the 300 m long pipes to and from the BTES causing too high computed underground temperatures at the end of the second year. Furthermore, it is not possible to install the BHE and the measuring lances absolutely vertical. Hence, an uncertainty of measurement due to inexact sensor positioning must be considered. The measured groundwater temperatures at GWM2a and GWM3a show an unexpected course in March 2010 and since end of June 2010 respectively. This may be explained by entering surface water into both wells.

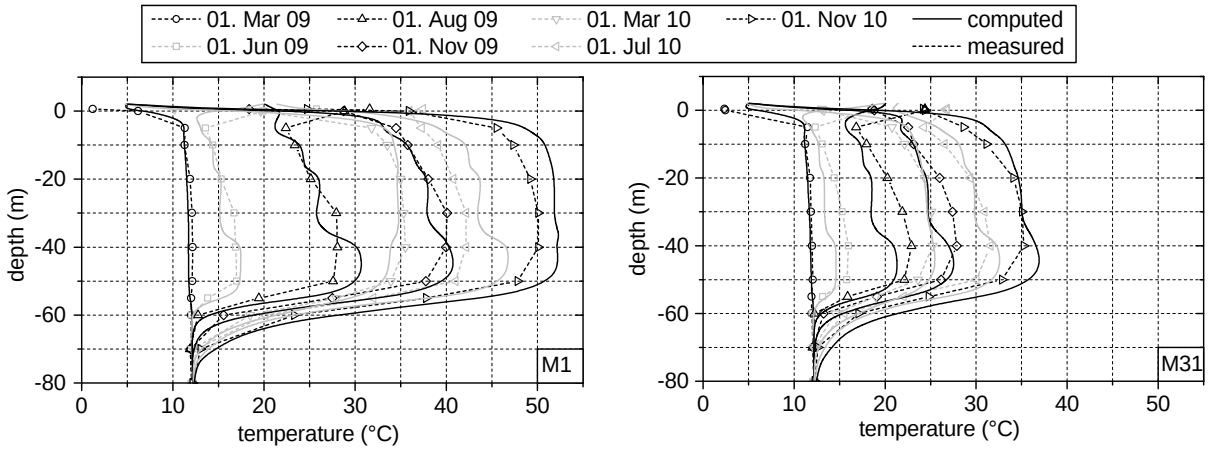

Figure 11: Measured and computed underground temperatures at measuring lance M1 (middle of BTES)

Figure 12: Measured and computed underground temperatures at measuring lance M31 (margin of BTES)

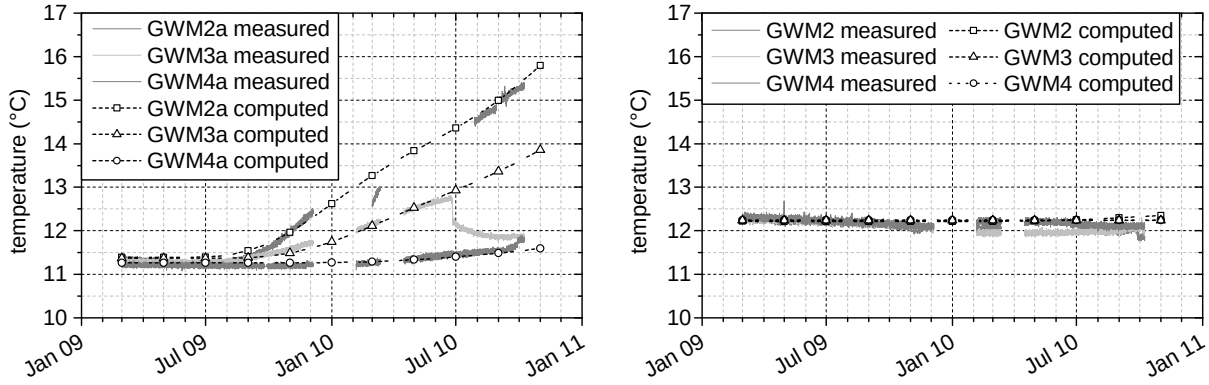

Figure 13: Measured and computed groundwater temperatures at wells GWM2a, GWM3a and GWM4a (all at 20 m depth)

Figure 14: Measured and computed groundwater temperatures at wells GWM2, GWM3 and GWM4 (all at 80 m depth)

4. Conclusions

The high accuracy of the newly developed FEFLOW simulation model for BTES is demonstrated by the validation against one analytical solution and measured data of two BTES with and without groundwater flow. It is shown that the simulation model is accurate enough for most engineering and scientific applications. The comparison to the analytical solution shows very similar results. In addition, the validation against measured data of the Neckarsulm BTES shows the high accuracy of the simulation model. Minor differences occurred when comparing the model with measured data of the BTES in Crailsheim. It is shown that these differences are predominantly caused by the uncertainty of the measured data and not by model deficiencies. In summary it can be concluded that the newly developed FEFLOW model is able to consider and calculate the influence of moving groundwater on the thermal behaviour of BHE and BTES in an appropriate and accurate manner.

5. References

[1] FEFLOW, Finite Element Subsurface Flow & Transport Simulation System, WASY GmbH, Berlin, Germany, 2007
[2] Diersch, H.-J.G.; Bauer, D.; Heidemann, W.; Rühaak, W.; Schätzl, P.: Finite element formulation for borehole heat exchangers in modeling geothermal heating systems by FEFLOW. FEFLOW White Papers Vol. V, DHI-WASY GmbH, Berlin, 2010.
[3] Diersch, H.-J.G.; Bauer, D.; Heidemann, W.; Rühaak, W.; Schätzl, P.: Finite element modeling of borehole heat exchanger systems - Part 1: Fundamentals. Computers & Geosciences 37 (2011) 1122–1135, DOI:10.1016/j.cageo.2010.08.003.
[4] Diersch, H.-J.G.; Bauer, D.; Heidemann, W.; Rühaak, W.; Schätzl, P.: Finite element modeling of borehole heat exchanger systems - Part 2: Numerical Simulation. Computers & Geosciences 37 (2011) 1136–1147, DOI:10.1016/j.cageo.2010.08.002.
[5] Bauer, D.; Heidemann, W.; Müller-Steinhagen, H.; Diersch, H.-J.G.: Thermal resistance and capacity models for borehole heat exchangers. Int. Journal of Energy Research 84 (2010) 612–623, DOI: 10.1002/er.1689.
[6] Sutton, M.; Nutter, D.; Couvillion, R.: A Ground Resistance for Vertical Bore Heat Exchangers With Groundwater Flow. Journal of Energy Resources Technology 25 (2003) 183–189.
[7] Su, D.; Diao, N.; Fang, Z.: An analytical solution of the temperature response in ground heat exchangers with groundwater advection. 6th International Symposium of Heat Transfer, Beijing, 2004.
[8] Diao, N.; Li, Q.; Fang, Z.: Heat transfer in ground heat exchangers with groundwater advection. International Journal of Thermal Science 43 (2004) 1203–1211.
[9] Seiwald, H.; Hahne, E.: Underground sesonal heat storage for a solar heating system in Neckarsulm/Germany. Terrastock, the 8th International Conference on Thermal Energy Storage, Stuttgart, 2000.
[10] Rieger, M.: Saisonaler Erdsonden-Wärmespeicher in Crailsheim. bbr Fachmagazin für Brunnen- und Leitungsbau 09/2008, 24–32.
[11] Chaudhry, M.A.; Zubair, S.M.: Generalized incomplete gamma functions with applications. Journal of Computational and Applied Mathematics 55 (1994), 99–124.
[12] Chaudrhy, M.A.; Temme, N.M.; Veling, E.J.M.: Asymptotics and closed form of a generalized incomplete gamma function. Journal of Computational and Applied Mathematics 67 (1996), 371–379.
[13] Meyer, J.: Untersuchung des Einflusses der geothermalen Bodenparameter auf den Speichernutzungsgrad eines Erdwärmesondenspeichers mit Hilfe der Finiten Element Methode. Diploma thesis at the technical University of Braunschweig, Institut für Grundbau und Bodenmechanik, 2004.
[14] Seiwald, H.; Hahne, E.: Das solar unterstützte Nahwärmeversorgungssystem mit Erdwärmesonden-Speicher in Neckarsulm. 2. Internationaler Kommunaler Klimaschutzkongreß Friedrichshafen, 1998.
[15] Benner, M.; Mahler, B.; Mangold, D.; Schmidt, T.; Schulz, M.; Seiwald, H.: Solar unterstützte Nahwärmeversorgung mit und ohne Langzeitwärmespeicher. Abschlussbericht zum BMBF-Forschungsvorhaben 0329606C (Sep. 1994 bis Okt. 1998), Stuttgart, 1999.
[16] Nußbicker-Lux, J.: Simulation und Dimensionierung solar unterstützter Nahwärmesysteme mit Erdsonden-Wärmespeicher. Dissertation Universität Stuttgart, 2010.
[17] Pahud, D.; Fromentin, A.; Hadorn, J.-C.: The Superposition Borehole Model for TRNSYS (TRNSBM). User Manuel, Internal Report, LASEN-EPFL, Lausanne, 1996.
[18] ANSYS: ANSYS® Multiphysics, Release 10.0, Documentation. ANSYS, Inc. Canonsburg, PA, 2005.
[19] Bauer, D.; Heidemann, W.; Marx, R.; Nußbicker-Lux, J.; Ochs, F.; Panthalookaran, V.; Raab, S., 2009: Solar unterstützte Nahwärme und Langzeit-Wärmespeicher (solar assisted district heating and seasonal thermal energy stores) . Forschungsbericht zum BMU-Vorhaben 0329607J (Juni 2005 bis Juli 2008), Stuttgart, Germany.
[20] Bauer, D.; Heidemann, W.; Müller-Steinhagen, H.; Diersch, H.-J.G.; Rühaak, W.; Schätzl, P.; Koller, B.; Sass, I.; Mielke, P.: Untersuchung des Einflusses von Grundwasserströmung auf Erdsonden-Wärmespeicher. Abschlussbericht zum BMU-Vorhaben FKZ 0329289A, Stuttgart, 2010.

6. Nomenklature

a	argument of Γ (-)
a_{eff}	effective thermal diffusivity ($m^2\ s^{-1}$)
c_p	specific heat capacity ($J\ kg^{-1}\ K^{-1}$)
b	argument of Γ (-)
d	diameter (m)
d_i	inner diameter of a U-tube (m)
d_o	outer diameter of a U-tube (m)
E_i	exponential integral function
${}_0F_1$	confluent hypergeometric function
Fo	Fourier number (-)
I_0	modified Bessel function of first kind of order zero
k	thermal conductivity ($W\ m^{-1}\ K^{-1}$)
L	length (m)
$\dot{m}$	mass flow rate ($kg\ s^{-1}$)
Pe	Péclet number (-)
$\dot{q}$	specific heat flow rate ($W\ m^{-1}$)
R_b	borehole thermal resistance ($m\ K\ W^{-1}$)
s	U-tube shank spacing (m)
t	time (s)
w	velocity ($m\ s^{-1}$)
w_a	groundwater pore velocity ($m\ s^{-1}$)
w_{DA}	Darcy velocity ($m\ s^{-1}$)
x, y	distance (m)
Γ	generalized incomplete gamma function
ϑ	Celsius temperature (°C)
$\vartheta_{s,0}$	initial underground temperature (°C)
ρ	density ($kg\ m^{-3}$)
Ω	porosity of the underground

Subscripts:

b	borehole (wall)
eff	effective
f	fluid
g	grouting material
p	pipe
s	soil

7. Acknowledgements

The scientific work has been supported by the German Federal Ministry for the Environment, Nature Conservation and Nuclear Safety. The authors gratefully acknowledge this support and carry the full responsibility for the content of this paper.